Biogeosciences, 21, 1887–1902, 2024
https://doi.org/10.5194/bg-21-1887-2024

Biogeosciences
Open Access
EGU

Simulated terrestrial runoff shifts the metabolic balance of a coastal Mediterranean plankton community towards heterotrophy

Tanguy Soulié[1], Francesca Vidussi[1], Justine Courboulès[1], Marie Heydon[1], Sébastien Mas[2], Florian Voron[2], Carolina Cantoni[3], Fabien Joux[4], and Behzad Mostajir[1]

[1]MARine Biodiversity, Exploitation and Conservation (MARBEC), Univ. Montpellier, CNRS, Ifremer, IRD, Montpellier, France
[2]MEDIterranean Platform for Marine Ecosystem Experimental Research (MEDIMEER), OSU OREME, Univ. Montpellier, INRAE, CNRS, IRD, Sète, France
[3]CNR-ISMAR, Instituto di Scienze Marine, Area Science Park, ed. Q2, Basovizza, Trieste, Italy
[4]Laboratoire d'Océanographie Microbienne (LOMIC), Observatoire Océanologique de Banyuls, CNRS, Sorbonne Université, Banyuls-sur-Mer, France

Correspondence: Tanguy Soulié (tanguy.soulie@gmail.com) and Behzad Mostajir (behzad.mostajir@umontpellier.fr)

Received: 22 November 2023 – Discussion started: 24 November 2023
Revised: 21 February 2024 – Accepted: 23 February 2024 – Published: 17 April 2024

Abstract. Climate change is projected to increase the frequency and intensity of extreme rainfall events in the Mediterranean region, increasing runoffs of terrestrial matter into coastal waters. To evaluate the consequences of terrestrial runoff for plankton key processes, an in situ mesocosm experiment was conducted for 18 d in the spring of 2021 in the coastal Mediterranean Thau Lagoon. Terrestrial runoff was simulated in replicate mesocosms by adding soil from an adjacent oak forest that had matured in water from the main tributary river of the lagoon. Automated high-frequency monitoring of dissolved oxygen, chlorophyll *a* fluorescence, salinity, light, and temperature was combined with manual sampling of organic and inorganic nutrient pools, pH, carbonate chemistry, and maximum quantum yield ($F_v : F_m$) of photosystem II (PSII). High-frequency data were used to estimate the gross primary production (GPP) of oxygen, community respiration (CR), and phytoplankton growth (μ) and loss (L) rates. During the first half of the experiment (d2–d11), the simulated runoff reduced light availability (−52 %), chlorophyll *a* concentrations (−70 %), and phytoplankton growth rates (−53 %). However, phytoplankton maintained a certain level of primary production by increasing its photosynthetic efficiency. Meanwhile, the runoff enhanced CR (+53 %), shifting the metabolic status (GPP : CR) of the system toward heterotrophy and increasing the partial pressure of carbon dioxide (pCO_2), potentially switching the direction of the air–sea CO_2 exchange. However, during the second part of the experiment (d11–d17), remineralized nutrients boosted phytoplankton growth (+299 %) in the terrestrial runoff treatment but not its loss rates, leading to phytoplankton biomass accumulation and suggesting a mismatch between phytoplankton and its predators. Our study showed that a simulated terrestrial runoff significantly affected key plankton processes, suggesting that climate-change-related increases in runoff frequency and intensity can shift the metabolic balance of Mediterranean coastal lagoons towards heterotrophy.

1 Introduction

Climate change is predicted to increase the frequency and intensity of short extreme rainfall events in the Mediterranean region (Alpert et al., 2002; Sanchez et al., 2004). Consequently, the runoff of terrestrial matter will become more frequent in coastal Mediterranean waters. These runoffs constitute a pulse input of organic and inorganic nutrients into the water column and decrease light penetration (Nunes et al., 2009), substantially impacting marine ecosystems and, notably, plankton communities (Deininger and Frigstad, 2019; Striebel et al., 2023).

Plankton is crucial for aquatic ecosystems because it forms the basis of the aquatic food web and plays an important role in multiple biogeochemical cycles, notably that of oxygen (Falkowski et al., 2003; Falkowski, 2012). Indeed, phytoplankton produces oxygen through its gross primary production (GPP), and all planktonic organisms consume it through aerobic community respiration (CR). Hence, assessing GPP and CR provides a community metabolism index (GPP : CR) and determines the capacity of an aquatic ecosystem to serve as a net producer or consumer of oxygen and as a sink or source of atmospheric carbon dioxide (Lopez-Urrutia et al., 2006). This community metabolism index considerably depends on the fate of phytoplankton, which is itself related to phytoplankton growth (μ) and loss (L) rates. Therefore, assessing μ and L provides a trophic index ($\mu : L$) related to the performance of both phytoplankton and its predators (Soulié et al., 2022a).

The consequences of terrestrial runoffs for plankton communities and associated processes remain unclear. The inputs of terrestrial carbon and nutrients have been shown to promote phytoplankton and bacteria in Mediterranean coastal waters (Pecqueur et al., 2011; Liess et al., 2016), possibly leading to higher GPP and CR. However, this positive effect of nutrient enrichment can be mitigated by light attenuation resulting from the runoff, which can depress phytoplankton photosynthesis and therefore GPP, as observed in the North Sea, Baltic Sea, and a North Atlantic bay (Mustaffa et al., 2020; Paczkowska et al., 2020; Soulié et al., 2022b). The contradictory effects of light attenuation and nutrient enrichment induced by terrestrial runoffs on plankton metabolism can change the structure of planktonic communities and, ultimately, their related processes. They can favour bacteria over phytoplankton (Meunier et al., 2017; Andersson et al., 2018; Courboulès et al., 2023) and large phytoplankton species at the expense of smaller cells (Deininger et al., 2016; Mustaffa et al., 2020) and decrease the abundance of protozooplankton (Courboulès et al., 2023). Consequently, these shifts can alter plankton processes because the structure and functions of aquatic communities are closely related (Giller et al., 2004).

Although the consequences of terrestrial runoffs have been well studied in freshwater systems, an important knowledge gap exists regarding the impacts of terrestrial runoffs on coastal marine ecosystems (Blanchet et al., 2022). In this regard, evaluating the consequences of terrestrial runoffs on plankton communities and processes in ecologically and economically important areas such as coastal lagoons (Soria et al., 2022), enclosed systems that are often subject to inputs from the land, is of fundamental concern. In the present study, we conducted an in situ mesocosm experiment in the Mediterranean coastal Thau Lagoon, a shallow productive lagoon which hosts oyster farms and serves as a nursery for several wild fish species (La Jeunesse et al., 2015). Moreover, it is naturally subjected to storm-induced terrestrial runoffs (Pecqueur et al., 2011; Fouilland et al., 2012), notably in fall during the Cévenol events, a meteorological phenomenon characterized by storms and heavy rainfalls that usually cause flash flooding on the Mediterranean coast (Ducrocq et al., 2008). Six mesocosms were used, with half serving as control mesocosms and with a terrestrial runoff simulated in the other half by adding soil from an adjacent typical Mediterranean oak forest that maturated over 2 weeks in water from the Vène River, the main river tributary of the Thau Lagoon (Plus et al., 2006). The responses of all plankton food web compartments in the present experiment have been detailed by Courboulès et al. (2023). In the present study, high-frequency data from automated sensors immersed in the mesocosms were used to estimate GPP, CR, μ, and L in each mesocosm and assess how both the metabolic and the trophic indices of the community responded to the simulated runoff. Manual sampling was performed to assess dissolved and particulate materials and photosynthetic efficiency and carbonate system parameters. We hypothesized that (1) the metabolic index would be shifted by the runoff towards heterotrophy through light reduction and inputs of organic matter and that (2) the terrestrial runoff would affect the trophic index by creating imbalance between phytoplankton and its factors of loss.

2 Material and methods

2.1 In situ mesocosm experimental setup

An in situ mesocosm experiment was performed for 18 d in May 2021 in the Thau Lagoon (France) using the facilities of the MEDIterranean platform for Marine Ecosystems Experimental Research (MEDIMEER; 43°24′53″ N, 3°41′16″ E). The duration of the experiment was set to 18 d in order to monitor the responses of plankton in the medium term (multiple days to weeks), as interesting dynamics were already reported in control treatments during previous experiments in the Thau Lagoon up to almost 3 weeks after the start of the experiment (Courboulès et al., 2021; Soulié et al., 2022a). However, the duration of the experiment was limited by COVID-19 pandemic restrictions, preventing the authors from conducting a longer experiment. The Thau Lagoon is a shallow coastal lagoon of 75 km^2 with a mean depth of 4 m and is located on the French coast of the northwestern Mediterranean Sea (Derolez et al., 2020a). Six mesocosms were deployed in the lagoon. Each mesocosm consisted of a bag, sealed at the bottom, made of nylon-reinforced 200 µm thick vinyl acetate–polyethylene film which was 3 m high and 1.2 m wide, resulting in a total volume of 2200 L (Insinööritoimisto Haikonen Oy, Sipoo, Finland). Each mesocosm was equipped with a sediment trap at the bottom. A schematic representation of the mesocosm setup can be found in Soulié et al. (2021) and in the Supplement. Each mesocosm was covered with a dome of polyvinyl chloride to avoid external inputs. On 3 May (d0), all the mesocosms were filled simultaneously using a pump (SXM2/A

SG; Flygt) with 2200 L of subsurface lagoon water preliminarily screened by filtering with a 1 mm mesh to remove large particles and organisms. The water was pooled in a large container before being distributed simultaneously by gravity to the six mesocosms through parallel pipes. In each mesocosm, the water column was continuously homogenized with a pump (Model 360; Rule) immersed at a depth of 1 m, resulting in a turnover rate of approximately 3.5 d^{-1}. Observations performed with a microscope indicated that organisms (phytoplankton and zooplankton), even fragile organisms such as ciliates, did not seem to be damaged by the mixing procedure. Three mesocosms served as controls, while in three others maturated soil was added on 4 May (d1) to simulate a terrestrial runoff event (these mesocosms are hereafter referred to as the terrestrial runoff treatment). Throughout the experiment, a total of 510 L was sampled from each mesocosm, representing 23 % of the initial volume of the mesocosms. For each treatment, one mesocosm displayed considerable differences in biological, physical, and chemical parameters compared to the two other replicates of the same treatment, most probably because of the malfunctioning of the mixing pumps, and it was therefore removed from the analysis. Data are therefore presented as the mean of the two replicates for each treatment ± the range of observations. Thus, any interpretation of the presented data must take into account the low number of replications and be done cautiously.

2.2 Soil extraction, preparation, and maturation

Soil was extracted 2 weeks before the beginning of the mesocosm experiment from the Puéchabon state forest, a fully preserved typical Mediterranean oak forest located approximately 30 km north of the Thau Lagoon (43°44′29″ N, 3°35′45″ E) (Allard et al., 2008). The soil was then roughly screened by sifting through a 1 cm mesh. On the same day as soil extraction was performed, water was collected from the Vène River, the main tributary of the Thau Lagoon, which is known for its episodic flash floods (Pecqueur et al., 2011). Water was screened by filtering with a 200 µm mesh to remove large particles and organisms. The soil and river water were then mixed to reach a concentration of 416 g soil L^{-1}, which represents natural flash flood events occurring in the lagoon (Fouilland et al., 2012). This mixture was then left to mature for 2 weeks in transparent Nalgene carboys placed in an outdoor pool continuously supplied with natural water from the Thau Lagoon. During the maturation step, each carboy was homogenized and aerated daily. This maturation was performed to mimic the degradation process of the most labile compounds that naturally occurs during their transportation from the soil to coastal waters during natural runoff events (Müller et al., 2018). After the manual mesocosm sampling on 4 May (d1), 7 L of the soil solution was added to each of the three "terrestrial runoff" mesocosms, representing a final concentration of 1.3 g soil L^{-1}. Further details regarding the choice and description of the soil addition protocol can be found in Courboulès et al. (2023).

2.3 Acquisition, calibration, and correction of the high-frequency sensor data

In each mesocosm, a set of high-frequency sensors was immersed to a depth of 1 m. Each set consisted of a fluorometer (ECO FLNTU; Sea-Bird Scientific, United States) which measured Chl *a* fluorescence, from which Chl *a* concentration was derived; an oxygen optode (3835; Aanderaa, Bergen, Norway) which measured dissolved oxygen (DO) concentration and saturation; an electromagnetic induction conductivity sensor (4319; Aanderaa, Bergen, Norway) which measured salinity; a spherical underwater quantum sensor (LI-193; LI-COR, United States) which measured the incident photosynthetically available radiation (PAR); and three water temperature probes (107 Temperature Probe; Campbell Scientific, United States) installed at three different depths (0.5, 1, and 1.5 m). Each sensor recorded measurements every minute during the entire experiment. In the "Results" section, the high-frequency data are presented as daily averages. The fluorometers, oxygen optodes, conductivity sensors, and temperature probes were calibrated before and after the experiment. In addition, Chl *a* fluorescence and oxygen sensor data were corrected using discrete high-performance liquid chromatography (HPLC) Chl *a* and Winkler DO measurements, respectively. To do so, three borosilicate bottles (120 mL) were filled with water sampled from each mesocosm using a 5 L Niskin water sampler at a depth of 1 m every other day in the morning. The DO measurement was immediately fixed by adding Winkler reagents (Carrit and Carpenter, 1966). After at least 6 h of fixation during which bottles were kept underwater and in the dark in opaque plastic tanks filled with freshwater at room temperature, the DO concentration in each bottle was measured with an automated Winkler titrator (Metrohm 916 Ti-Touch) using a potentiometric titration method. Similarly, a polycarbonate bottle (2 L) was filled with water that was sampled every morning from each mesocosm using a Niskin water sampler at a depth of 1 m. Samples were then immediately filtered under low-light conditions using a vacuum pump on glass-fibre filters (Whatman GF/F; 0.7 µm pore size). Filters were then stored at −80 °C until analyses with HPLC (Shimadzu) were conducted following the method of Zapata et al. (2000). The HPLC was composed of a pump (DGU-405; Shimadzu), an automatic injector (LC-40D; Shimadzu), a Peltier oven (CTO-40S; Shimadzu), a PDA detector (SPD-M40; Shimadzu), and a fluorimeter detector (RF-20A; Shimadzu). The stationary phase used is a C8 column (SunFire C8; Waters) with a C8 column guard (Waters). Details of the calibration procedure can be found in the Supplement and in Soulié et al. (2023).

2.4 Manual mesocosm sampling and monitoring for chemical variables

Each mesocosm was sampled daily using a 5 L Niskin water sampler at a depth of 1 m to monitor dissolved inorganic nutrients (nitrate and nitrite, $NO_2^- +$ and NO_3^-; ammonium, NH_4^+; and orthophosphate, PO_4^{3-}), dissolved organic carbon (DOC), and particulate organic carbon (POC) and nitrogen (PON) concentrations; they were sampled every second day to measure pH and total alkalinity (TA). For dissolved inorganic nutrient analyses, 50 mL subsamples of mesocosm water were placed in acid-washed polycarbonate bottles. Directly after, these samples were filtered over 0.45 µm filters (Gelman Sciences, United States) and stored in high-density polyethylene tubes at −20 °C until further analyses that were performed within 48 h. Nitrate, nitrite, and orthophosphate analyses were performed with an automated colourimeter (Skalar Analytical B.V., the Netherlands; Aminot and Kérouel, 2007), and ammonium analyses were performed using the fluorometric method (module 7200-067-W; Turner Design, United States; Aminot et al., 1997; Holmes et al., 1999). For DOC analyses, 30 mL subsamples of mesocosm water were filtered through two pre-combusted (4 h, 450 °C) glass-fibre filters (Whatman GF/F); 90 µL of phosphoric acid (85 % concentration) was then added, and subsamples were then stored at 4 °C in the dark pending analyses, which were performed by high-temperature catalytic oxidation (HTCO) on a total organic carbon analyser (TOC-LCSH; Shimadzu). For POC and PON analyses, subsamples (0.5–1 L) of mesocosm water were filtered over pre-combusted (4 h; 450 °C) glass-fibre filters (Whatman GF/F). Filters were then placed in a stove at 60 °C for at least 12 h. The POC and PON concentrations were then measured using a CHN analyser (UNICUBE; Elementar). The samples for pH and TA determinations were collected in 300 mL borosilicate glass bottles according to standard sampling methods for carbonate chemistry (Dickson et al., 2007). Samples for TA determination were filtered immediately on glass-fibre filters (Whatman GF/F; 0.45 µm pore size), spiked with 50 µL of $HgCl_2$-saturated solution, and stored for later analysis. Samples for pH analysis were spiked with $HgCl_2$ and were analysed within 36 h.

pH was measured spectrophotometrically (LAMBDA 365 UV/Vis; PerkinElmer) on a "total scale" at 25.0 °C (pH_{25}) with *m*-cresol purple (*m*-Cp) as an indicator (reproducibility ± 0.002) and thermostated cells (10 cm optical path; 28 mL), according to Clayton and Byrne (1993) and Dickson et al. (2007), with duplicate analysis for control and triplicate for treated mesocosms. TA was measured in the laboratories of the Institute of Marine Sciences of the National Research Council of Italy (CNR-ISMAR) in Trieste (duplicate analysis) using an open-cell potentiometric titration with a derivative determination of the end point, according to Hernández-Ayon et al. (1999) (reproducibility ± 0.1 µmol kg^{-1}). Certified reference seawater for carbonate chemistry (provided by Andrew Dickson, Scripps, California) was used for TA analysis and to check the stability of the pH analysis during the experiment. After the experiment, the *m*-Cp used was checked against a purified *m*-Cp batch (Liu et al., 2011), showing a difference of < 0.005 pH units. The dissolved inorganic carbon (DIC) concentration, CO_2 partial pressure (pCO_2), and pH at in situ temperature (pH) were calculated using the CO2SYS program (Microsoft Excel version 2.5; Lewis and Wallace, 1998; Pierrot et al., 2006) and using the carbonate constants from Lueker et al. (2000), sulfate constants from Dickson (1990), and parameterization of borate from Lee et al. (2010).

2.5 Estimation of the daily light integral from the high-frequency PAR sensor data

PAR measurements were used to calculate the daily light integral (DLI). This value corresponds to the average quantity of light available for photosynthesis received by a 1 m^2 surface over a 24 h period (Soulié et al., 2022b). DLI was calculated using Eq. (1) as follows:

$$\mathrm{DLI} = \frac{\text{mean PAR} \times \text{day length} \times 3600}{1 \times 10^6}, \quad (1)$$

where DLI is expressed in mol m^{-2} d^{-1}, mean PAR between sunrise and sunset in µmol m^{-2} s^{-1}, and day length in hours.

2.6 Estimation of μ and L from the high-frequency Chl *a* sensor data

The high-frequency Chl *a* data were used to estimate phytoplankton growth (μ) and loss (L) rates following a method detailed by Soulié et al. (2022a). First, the high-frequency Chl *a* data were corrected for non-photochemical quenching as detailed in the Supplement. Then, each Chl *a* cycle was separated into an "increasing period" and a "decreasing period". The increasing period lasted from sunrise until the maximum Chl *a* fluorescence was reached, generally a few minutes to a few hours after sunset. The decreasing period lasted from this maximum until the next sunrise. For each period, an exponential fit was applied to the Chl *a* data, and L was estimated from the decreasing period. Then, μ was estimated from the increasing period. The detailed calculations are presented in the Supplement.

2.7 Estimation of GPP and CR from the high-frequency DO sensor data

DO data were used to estimate daily GPP and CR during the day (CRdaytime) and the night (CRnight), and daily CR was estimated following the method detailed by Soulié et al. (2021). This method is derived from the free-water diel oxygen technique (Staehr et al., 2010) and was specially developed for mesocosm experiments and to consider variability in both the coupling between day–night and DO cycles

and the respiration occurring during the day and at night. Briefly, each DO cycle was separated into a "positive instantaneous net community production period" (during which DO increases) and a "negative instantaneous net community production period" (during which DO decreases). For each period, the DO was smoothed using a five-point sigmoidal model. These smoothed data were then used to estimate oxygen metabolic parameters in two major steps. First, the oxygen exchange term between water and the atmosphere was calculated, taking into consideration its dependence on temperature and salinity. Then, instantaneous and daily metabolic parameters were estimated. A precise description of the method is provided by Soulié et al. (2021) and in the Supplement.

2.8 Maximum photosystem II quantum yield measurements

Phytoplankton photosynthetic performance was estimated based on the fluorescence of the photosystem II (PSII). Subsamples of 1.5 mL from the Niskin water sampler were collected daily and analysed using a portable pulse amplitude modulation fluorometer (AquaPen-C AP 110-C; Photon Systems Instruments, Czech Republic). The maximum quantum yield of photosynthesis ($F_v : F_m$) was measured after a 30 min acclimation period in the dark to ensure that all photosystem II reactional centres were open. The measurement was done using the "OJIP" protocol and an excitation wavelength of 450 nm (Strasser et al., 2000).

2.9 Heterotrophic bacterial abundance measurements

Heterotrophic bacterial abundance was assessed daily using flow cytometry. For this purpose, 1.5 mL samples were collected from the Niskin water sampler and fixed using glutaraldehyde (Grade I; Sigma-Aldrich; 4 % final dilution) and then frozen into liquid nitrogen before being maintained at −80 °C until further analyses. The samples were stained with SYBR Green I (S7563; Invitrogen; 0.25 % final dilution) (Marie et al., 1997). Analyses were performed using a FACSCanto2 flow cytometer (Becton Dickinson; set to low speed for 3 min), and internal cell size standards (cytometry fluorescent beads; Polysciences, Inc.) of 1 and 2 µm diameter were added to each run. Bacterial populations were identified and counted via stained green fluorescence (530 nm) and relative side scatter (Courboulès et al., 2021, 2023).

2.10 Statistical analyses

To test the difference between the control and the terrestrial runoff treatments, we performed repeated-measures analyses of variance (RM-ANOVAs) with the treatment as a fixed factor and time as a random factor (*nlme* package, R software) over the entire experiment (after the addition of soil, d2–d18) and over shorter periods to assess specific trends. Data from d1 were not included in the statistical analyses as sampling was performed before adding the soil, simulating the terrestrial runoff, in the runoff mesocosms. Statistical significance was set at $p < 0.05$. Before performing the RM-ANOVAs, the assumptions of homoscedasticity and normality were checked using the Levene and Shapiro–Wilk tests, respectively. When these assumptions were not met even after transforming the data (using a log or square-root transformation), a non-parametric Kruskal–Wallis test was performed instead of RM-ANOVA. The non-parametric Spearman's correlation coefficient was used to assess significant ($p < 0.05$) relationships between the logarithms of the response ratio (LRRs) of the variables. All data management and statistical analyses were performed using the R software (version 4.0.1).

3 Results

3.1 Effects of the terrestrial runoff treatment on physical and chemical conditions

In the control treatment, the water temperature varied from 16.68 ± 0.16 to 17.95 ± 0.65 °C (Fig. 1a) and was not significantly different in the terrestrial runoff treatment compared to the control (Table 1). The salinity was on average 38.42 ± 0.11 in the control treatment, increasing almost continuously throughout the experiment (Fig. 1b). In the terrestrial runoff treatment, the salinity was significantly reduced by 0.7 % (Table 1). Similarly, the DLI was, on average, 18.65 ± 1.45 mol m^{-2} d^{-1} in the control treatment (Fig. 1c). The terrestrial runoff drastically decreased it by 76 % on d2 and by, on average, 43 % over the entire experiment. This negative effect was stronger during the first half of the experiment (52 % from d2–d11) and was attenuated during the second half of the experiment (27 % from d12–d18) (Table 1). In the control treatment, pH varied between 8.10 ± 0.05 and 8.19 ± 0.01 (Fig. 1d), decreasing from d1 to d10 before stabilization until the end of the experiment. In the runoff treatment, it was significantly reduced by, on average, 0.03 units (8.06 ± 0.01 to 8.19 ± 0.01 in the runoff treatment) (Table 1). In addition, pCO_2 ranged from 292.49 ± 0.45 to 368.27 ± 43.97 µatm in the control treatment (Fig. 1e). In the runoff treatment, it was significantly higher by 9 % compared to the control despite returning to the control level by the end of the experiment (Table 1). DIC concentrations ranged from 2184.04 ± 14.89 to 2230.44 ± 0.76 µmol kg^{-1} (Fig. 1f). They were significantly higher by 1 % in the runoff treatment than in the control, with the highest difference between treatments on d2 (3 %) (Table 1). DOC concentrations were on average 1.70 ± 0.10 mg L^{-1} in the control treatment (Fig. 1g). In the terrestrial runoff treatment, DOC concentrations were not immediately enhanced after the addition of soil, reaching higher concentrations than in the control only in the middle and at the end of the experiment. However, no significant

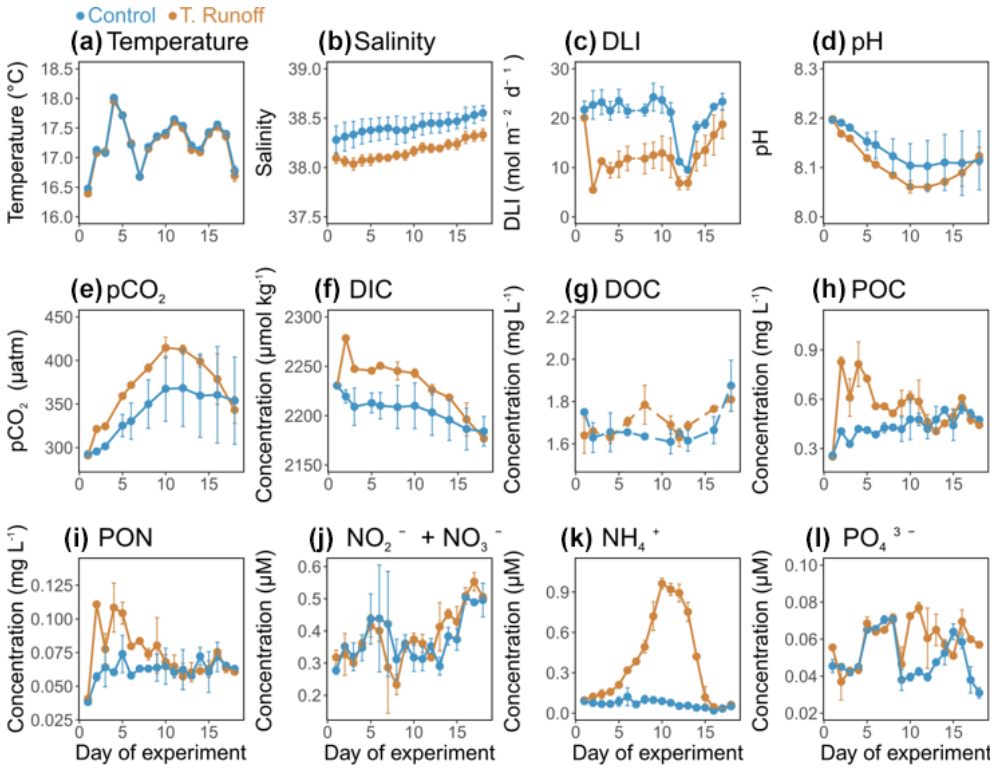

Figure 1. Daily average **(a)** temperature, **(b)** salinity, **(c)** daily light integral (DLI), **(d)** pH, **(e)** pCO_2, **(f)** dissolved inorganic carbon concentration (DIC), **(g)** dissolved organic carbon concentration (DOC), **(h)** particulate organic carbon concentration (POC), **(i)** particulate organic nitrogen concentration (PON), **(j)** nitrate and nitrite concentration ($NO_2^- + NO_3^-$), **(k)** ammonium concentration (NH_4^+), and **(l)** orthophosphate concentration (PO_4^{3-}) in the control (blue) and terrestrial runoff (gold) treatments. Error bars represent the range of the observations (min and max values).

differences were observed between the treatments (Table 1). POC and PON concentrations displayed similar dynamics over time. POC concentrations ranged from 0.26 ± 0.01 to $0.55 \pm 0.09\,\mathrm{mg\,L^{-1}}$ (Fig. 1h), whereas PON concentrations ranged from 0.04 ± 0.01 to $0.07 \pm 0.01\,\mathrm{mg\,L^{-1}}$ (Fig. 1i). They were both significantly enhanced by 32 %–50 % by the terrestrial runoff at the beginning of the experiment (d2–d12), then decreased to the level of the control (Table 1). The concentrations of dissolved inorganic nutrients exhibited different trends. Nitrate and nitrite concentrations ranged from 0.29 ± 0.03 to $0.50 \pm 0.01\,\mu\mathrm{M}$ in the control treatment and were not significantly affected by the terrestrial runoff (Fig. 1j, Table 1). Conversely, while ammonium concentrations remained rather constant in the control treatment during the experiment, ranging from 0.02 ± 0.01 to $0.12 \pm 0.07\,\mu\mathrm{M}$, they increased significantly in the terrestrial runoff treatment, reaching $0.96 \pm 0.04\,\mu\mathrm{M}$ on d10 before decreasing to the control level on d16 (Fig. 1k; Table 1). Orthophosphate concentrations ranged from 0.03 ± 0.01 to $0.07 \pm 0.01\,\mu\mathrm{M}$ in the control treatment, with peaks at the beginning and the end of the experiment (Fig. 1l). They were significantly higher in the terrestrial runoff treatment but only in the middle of the experiment (63 % from d10–d13) (Table 1).

3.2 Effects of the terrestrial runoff treatment on bacterial abundances

In the control treatment, bacterial abundances ranged from $0.8 \times 10^6 \pm 0.3 \times 10^6$ to $1.9 \times 10^6 \pm 0.8 \times 10^6$ cells $\mathrm{mL^{-1}}$ (Fig. 2). They were significantly higher in the terrestrial runoff treatment from d2–d8 (59 %) and from d15–d18 (51 %), whereas they were significantly lower in the middle of the experiment (−47 % from d9–d14) (Table 1). As a consequence, no significant differences were observed when considering the entire duration of the experiment.

3.3 Effects of the terrestrial runoff treatment on phytoplankton: Chl *a* and growth and loss rates

In the control treatment, the Chl *a* concentrations ranged from 0.83 ± 0.30 to $1.91 \pm 0.45\,\mathrm{\mu g\,L^{-1}}$ (Fig. 3a). They remained rather constant during the first half of the experiment before increasing from d11 to d13 and then decreasing until the end of the experiment. In the terrestrial runoff treatment, they were significantly lower than in the control, particularly during the first part of the experiment (−70 % from d2–d11) (Table 1). However, at the end of the experiment, they in-

Table 1. Summary table of the statistical comparison and the relative change between the terrestrial runoff and the control treatments in percentages. The significance level was set to 0.05 and significant p values and their corresponding relative changes are highlighted in bold. When an RM-ANOVA was performed, its F value is given in brackets, and when a Kruskal–Wallis was performed instead, this is indicated with KW.

Parameter	Period	p value	% difference
Temperature	2–18	0.64 (KW)	−0.2
Salinity	2–18	$< 1 \times 10^{-4}$ ($F_{1,16} = 1035$)	−0.7
	2–18	1.4×10^{-3} (KW)	−43.3
DLI	2–11	9.1×10^{-4} (KW)	−51.6
	12–18	1.4×10^{-3} ($F_{1,6} = 32.9$)	−27.3
pH	2–18	3×10^{-4} ($F_{1,9} = 32.4$)	−0.4
pCO_2	2–18	4×10^{-4} ($F_{1,9} = 30.5$)	8.9
DIC	2–18	7×10^{-4} ($F_{1,9} = 25.3$)	1.3
DOC	2–18	0.27 (KW)	0.4
	2–18	2.2×10^{-6} ($F_{1,16} = 11.5$)	27.8
POC	2–12	1.1×10^{-8} ($F_{1,10} = 27.9$)	49.3
	12–18	0.621 (KW)	−2.0
	2–18	0.001 (KW)	18.8
PON	2–12	1.6×10^{-5} ($F_{1,10} = 12.9$)	32.3
	12–18	0.474 ($F_{1,6} = 0.7$)	−2.7
$NO_2^- + NO_3^-$	2–18	0.75 ($F_{1,16} = 0.1$)	1.3
NH_4^+	2–18	3.2×10^{-4} (KW)	486.5
PO_4^{3-}	2–18	0.02 ($F_{1,16} = 6.8$)	18.0
	10–13	8.4×10^{-3} ($F_{1,3} = 38.7$)	62.7
	2–18	0.183 (KW)	15.0
Bacterial abundances	2–8	1.3×10^{-4} ($F_{1,6} = 37.2$)	59.0
	9–14	2.5×10^{-3} ($F_{1,5} = 24.2$)	−47.0
	15–18	6.7×10^{-3} ($F_{1,3} = 22.7$)	51.0
	2–18	1.2×10^{-3} ($F_{1,17} = 14.9$)	−30.2
Chl a	2–11	1.6×10^{-4} (KW)	−70.2
	12–18	0.89 ($F_{1,8} = 0.02$)	4.2
	2–17	0.86 ($F_{1,15} = 0.03$)	110.6
Growth rate (μ)	2–11	0.02 ($F_{1,8} = 7.5$)	−52.8
	12–17	3.0×10^{-4} ($F_{1,5} = 77.9$)	298.7
Loss rate (L)	2–17	4.7×10^{-3} ($F_{1,15} = 11$)	−32.1
	3–14	6×10^{-4} ($F_{1,11} = 22.3$)	−60.0
$\mu : L$ ratio	2–17	0.02 ($F_{1,15} = 7.3$)	305.4
	11–18	1×10^{-4} ($F_{1,5} = 115$)	550.3
	2–17	0.37 (KW)	16.1

Table 1. Continued.

Parameter	Period	p value	% difference
GPP	9–14	1.1×10^{-3} ($F_{1,5} = 44.7$)	36.6
	12–17	0.08 ($F_{1,15} = 4.8$)	24.5
GPP : Chl a	2–17	0.02 (KW)	312.1
CR	2–17	$< 1 \times 10^{-4}$ ($F_{1,15} = 38.4$)	45.7
	2–11	2×10^{-4} ($F_{1,10} = 32.7$)	52.5
GPP : CR	2–17	7×10^{-4} ($F_{1,15} = 18.4$)	−17.6
	2–10	$< 1 \times 10^{-4}$ ($F_{1,15} = 82.5$)	−432
$F_v : F_m$	2–17	0.94 ($F_{1,17} = 0.01$)	0.4
	8–11	3.7×10^{-3} ($F_{1,5} = 68.7$)	43.0
CR : Chl a	2–17	7.5×10^{-4} (KW)	419.9
CR : Bacteria	2–17	0.16 (KW)	26.9
	9–14	2×10^{-4} ($F_{1,5} = 22.1$)	154.2

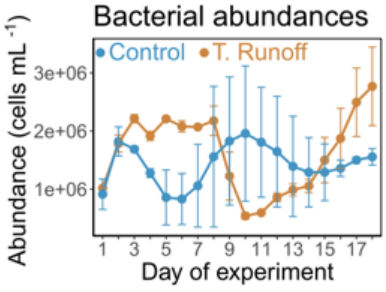

Figure 2. Daily average bacterial abundances in the control (blue) and terrestrial runoff (gold) treatments. Error bars represent the range of the observations (min and max values).

creased rapidly from d11–d15, even surpassing the control level.

In the control, μ ranged from 0.06 ± 0.04 to $0.64 \pm 0.06\,d^{-1}$, peaking on d4, d7, and d12 (Fig. 3b). In the terrestrial runoff treatment, it was significantly lower than in the control by an average of 53 % from d2–d10 (Table 1). However, it increased drastically during the second half of the experiment and was significantly almost 3 times higher than in the control from d12–d17. The value of L varied from 0.19 ± 0.12 to $0.95 \pm 0.05\,d^{-1}$ in the control treatment and was rather constant (Fig. 3c). In the terrestrial runoff treatment, it was significantly lower than in the control by an average of 32 % throughout the experiment and by an average of 60 % from d3–d14 (Table 1). However, it was higher than in the control from d2–d3 and came back to the control level at the end of the experiment. As a consequence of the generally higher L than μ in the control, the $\mu : L$ ratio was below 1 on 13 out of the 16 d (Fig. 3d). It ranged from 0.10 ± 0.06 to 2.76 ± 2.26. The terrestrial runoff significantly increased the $\mu : L$ ratio by an average of 305 % over the entire experiment (Table 1). The greatest difference between treatments was found on d13, when the ratio was almost 11 times higher in the terrestrial runoff than in the control treatment.

3.4 Effects of the terrestrial runoff treatment on primary production, respiration, and photosynthetic efficiency

In the control treatment, GPP ranged from 0.26 ± 0.02 to $0.78 \pm 0.03\,g\,O_2\,m^{-3}\,d^{-1}$ (Fig. 4a). After decreasing from d1–d2, it increased until it reached its maximum on d7 and then decreased almost continuously until the end of the experiment. In the terrestrial runoff treatment, it increased significantly by an average of 37 % at the middle of the experiment, from d9–d14 (Table 1). When the GPP was normalized by the daily Chl a concentration, it was significantly higher in the terrestrial runoff treatment than in the control by an average of 312 % throughout the experiment (Fig. 4b).

In the control treatment, CR ranged from 0.18 ± 0.01 to $0.67 \pm 0.02\,g\,O_2\,m^{-3}\,d^{-1}$, and it showed a similar dynamic as GPP (Fig. 4c). It was significantly enhanced in the terrestrial runoff treatment by an average of 46 % over the entire experiment (Table 1).

The GPP : CR ratio ranged from 0.94 ± 0.12 to 1.69 ± 0.19 in the control treatment, and it was higher than 1 on 16 out of 17 d (Fig. 4d). In the terrestrial runoff treatment, it decreased significantly by an average of 32 % during the first half of the experiment (d2–d10) before increasing and reaching the control level during the second half of the experiment (Table 1). Consequently, it was higher than 1 only on 10 out of the 17 d.

In the control, the maximum PSII quantum yield, an indicator of the maximum potential photosynthetic capacity, ranged from 0.24 ± 0.01 to 0.55 ± 0.04 (Fig. 4e). It was not significantly different between the treatments over the entire

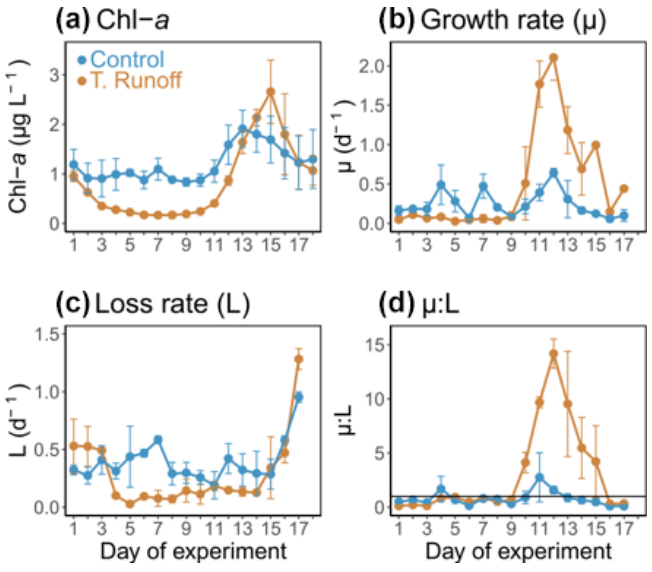

Figure 3. Daily average **(a)** chlorophyll *a* (Chl *a*), **(b)** phytoplankton growth rate (μ), **(c)** phytoplankton loss rate (L), and **(d)** growth : loss ratio ($\mu : L$) in the control (blue) and terrestrial runoff (gold) treatments. Error bars represent the range of the observations (min and max values). Note that μ and L could not be estimated on d18 owing to the lack of a complete fluorescence cycle.

experiment; however, it increased significantly by 43 % in the terrestrial runoff treatment from d8–d11 (Table 1).

When the CR was normalized by the daily Chl *a* concentration, it was significantly higher in the terrestrial runoff treatment than in the control by an average of 420 % throughout the experiment (Fig. 4f).

Finally, when CR was normalized by total bacterial abundance (Fig. 4g), it was not significantly different between treatments apart from d9–d14 when it was significantly higher by an average of 154 % in the terrestrial runoff treatment than in the control (Table 1).

3.5 Correlation matrix between the responses of phytoplankton processes, community metabolism, and environmental variables

To assess the relationships between the effects of the terrestrial runoff on various variables, Spearman's correlations were calculated between the LRRs of phytoplankton processes, community metabolism, and environmental variables. All significant correlations are shown in the matrix (Fig. 5). GPP was positively correlated with NH_4^+ and PO_4^{3-} concentrations and negatively correlated with bacteria abundance and POC and PON concentrations. CR was positively correlated with pCO_2 and POC and PON concentrations, while being negatively correlated with μ, Chl *a*, salinity, DLI, and pH. In addition, μ was positively correlated with L, Chl *a*, salinity, DLI, and $NO_2^- + NO_3^-$ and negatively with bacterial abundances and POC and PON concentrations. Similarly, L was positively correlated with Chl *a* and salinity and negatively correlated with pCO_2. In addition, Chl *a* was positively correlated with salinity, DLI, and $NO_2^- + NO_3^-$ and negatively correlated with POC and PON, while bacterial abundances were positively correlated with DOC and negatively correlated with NO_2^- and NO_3^-, NH_4^+, and PO_4^{3-}. Among environmental variables, it should be noted that DLI and POC and PON concentrations were negatively correlated and NH_4^+ and PO_4^{3-} were positively correlated.

4 Discussion

4.1 The terrestrial runoff depressed phytoplankton processes and shifted the metabolic balance of the system towards heterotrophy during the first half of the experiment

The present study aims to evaluate the effects of a simulated terrestrial runoff on key plankton processes in a coastal Mediterranean lagoon. During the first half of the experiment (d2–d11), the simulated terrestrial runoff strongly decreased available light (−52 %), consequently depressing phytoplankton biomass (−70 %) and growth rate (−53 %), as highlighted by the strong positive correlations among light availability, Chl *a*, and phytoplankton growth. The phytoplankton community investigated in the present study was typical of the Thau Lagoon in spring (Trombetta et al., 2019), mainly composed of diatoms, cryptophytes, and small nano- and picophytoplankton (Courboulès et al., 2023). The negative effect of light limitation induced by the runoff on phytoplankton biomass is consistent with a mesocosm experiment performed in the Baltic Sea, where terrestrial organic matter addition reduced phytoplankton biomass through light attenuation (Mustaffa et al., 2020), and, generally, with a meta-analysis conducted on 108 studies reporting an average 23 % reduction in photoautotroph biomass in response to experimentally reduced light across various freshwater and coastal ecosystems (Striebel et al., 2023). However, in the Thau Lagoon, a previous experiment reported a positive effect of soil addition, simulating a terrestrial runoff, on phytoplankton (Deininger et al., 2016). Nevertheless, the sinking of the added soil during the experiment performed by Deininger et al. (2016), despite the use of a mixing pump to limit sedimentation, might have rapidly lessened light attenuation, possibly releasing phytoplankton from the negative effect of light limitation. In addition, the experiment was conducted in late spring and early summer, when in light-oversaturated conditions (Trombetta et al., 2019), whereas our experiment was performed in spring, when light could be limiting for phytoplankton metabolism. Finally, Deininger et al. (2016) used a resin in their soil extraction procedure, yielding higher inorganic and organic nutrient concentrations in their extract compared to the protocol performed in the present study but

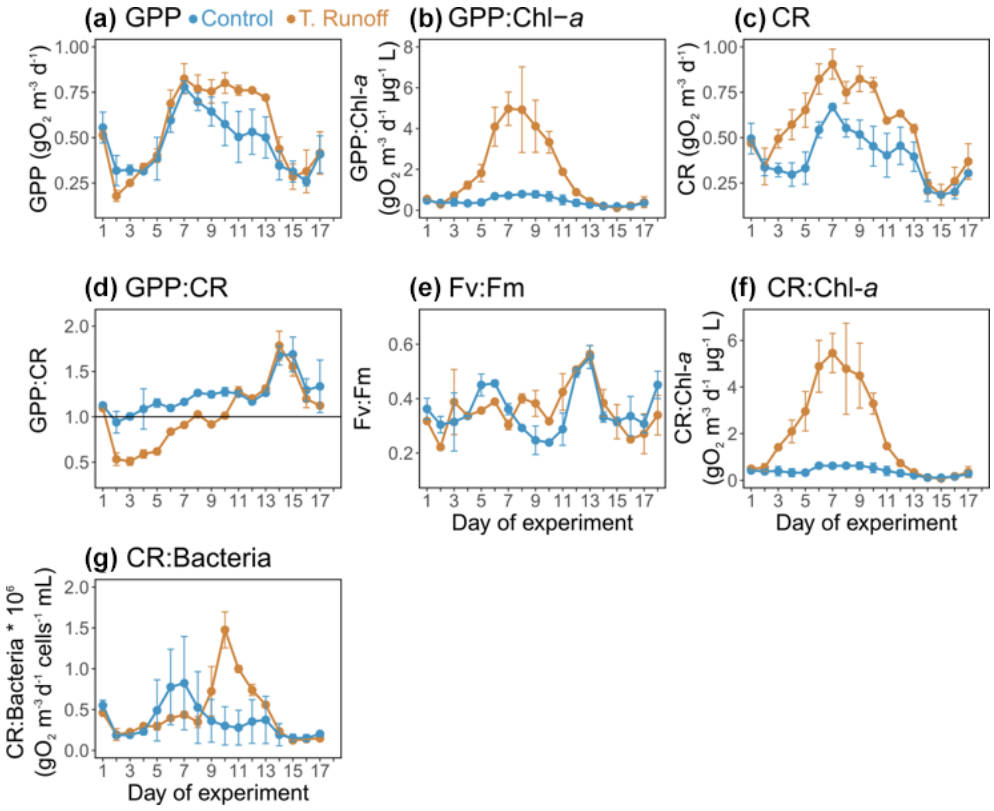

Figure 4. Daily average **(a)** gross primary production (GPP), **(b)** GPP normalized by chlorophyll *a* (GPP : Chl *a*), **(c)** community respiration (CR), **(d)** GPP : CR ratio, **(e)** maximum quantum yield ($F_v : F_m$) of photosystem II (PSII), **(f)** CR normalized by chlorophyll *a* (CR : Chl *a*), and **(g)** CR normalized by bacterial abundance (CR : bacteria) in the control (blue) and terrestrial runoff (gold) treatments. Error bars represent the range of the observations (min and max values). Note that GPP and CR could not be estimated on d18 owing to the lack of a complete oxygen cycle.

being farther from natural terrestrial runoffs (Scharnweber et al., 2021). In the present experiment, the maturation step aimed at mimicking processes which naturally occur during the transportation of soil to coastal waters during terrestrial runoffs, such as the degradation of the most labile organic compounds (Müller et al., 2018). The 14 d maturation period can be considered a long residence time in river water, regarding the fact that flash floods in the Mediterranean region are usually faster. Therefore, it can be supposed that the terrestrial matter added in the present study contained lower levels of labile organic compounds than what can be found during flash floods. This emphasizes the need for extreme caution when comparing experimental studies investigating terrestrial runoff effects because protocols often differ from one study to another.

In the present study, the lower phytoplankton biomass and growth rate in the runoff treatment were coupled with an overall decrease in phytoplankton loss rate from d3 until d14 (−60 %). Phytoplankton loss could be caused by multiple factors that occur concomitantly, including grazing by predators, viral lysis, sedimentation, and natural death (Landry and Hassett, 1982; Brussaard, 2004). As the terrestrial runoff induced a negative effect on phytoplankton biomass during the first half of the experiment, it may have led to lower prey availability for its predators, resulting in a lower phytoplankton loss rate. This is supported by the negative effect of the simulated runoff on protozooplankton abundances reported in the present experiment (Courboulès et al., 2023), which may be due to both lower phytoplankton abundance and higher grazing pressure from metazooplankton. Finally, the lower phytoplankton loss rate suggests that terrestrial runoffs could have important consequences for the entire plankton food web of coastal Mediterranean waters by disrupting phytoplankton loss processes, including grazing, which is the first link in the herbivorous food web (Legendre and Rassoulzadegan, 1995; Mostajir et al., 2015).

In contrast to phytoplankton biomass and growth, the gross primary production returned quickly to the control level (d4) and was even enhanced by the terrestrial runoff after a few days. This result was unexpected considering that oxygen production strongly depends on light, which was reduced by the runoff. However, we showed that the ratio of primary production to Chl *a* increased by more than 3 times in the runoff treatment, suggesting a strong enhancement of the

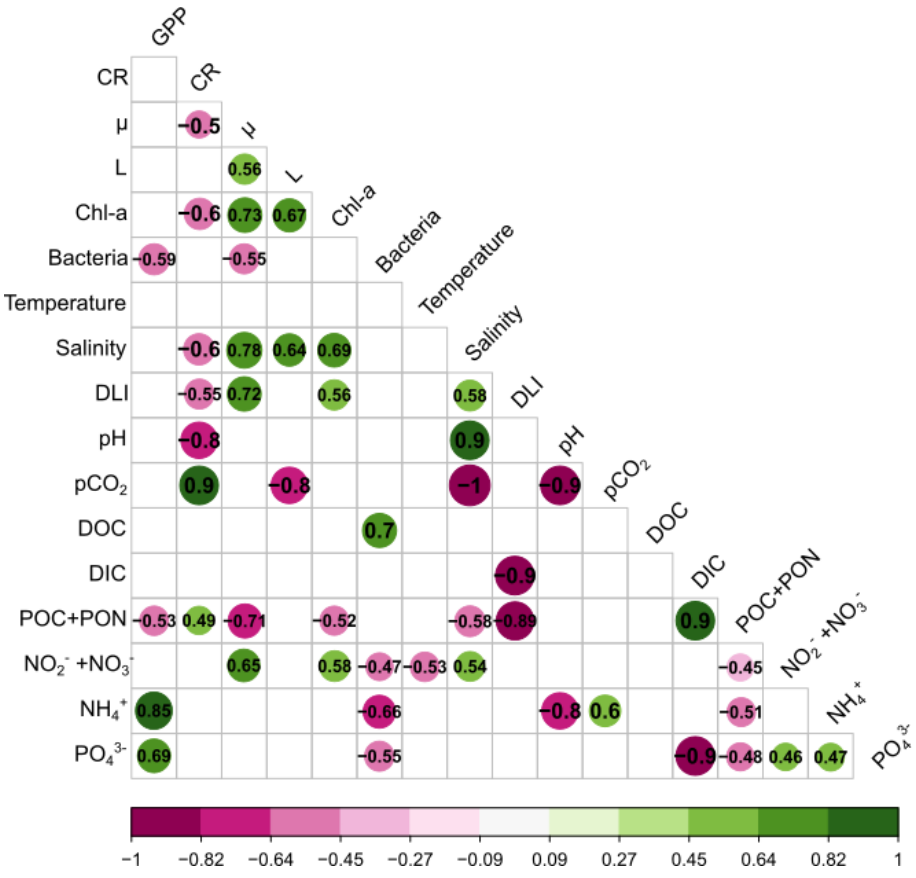

Figure 5. Correlation matrix based on Spearman's correlations between the log response ratio (LRR) of phytoplankton processes, community metabolism, and environmental variables. Only significant ($p<0.05$) correlations are shown in the matrix. Green illustrates positive correlations and purple negative correlations. (GPP: gross primary production; CR: respiration; μ: growth rate; L: loss rate; Chl a: chlorophyll a; Bacteria: bacterial abundance; DLI: daily light integral; pCO_2: partial pressure of CO_2; DOC: dissolved organic carbon; DIC: dissolved inorganic carbon; POC and PON: particulate organic carbon and nitrogen; NO_2^- and NO_3^-: nitrite and nitrate concentrations; NH_4^+: ammonium concentration; PO_4^{3-}: orthophosphate concentration.)

phytoplankton photosynthetic efficiency to cope with lower light availability. Supporting this, the maximum PSII quantum yield, an indicator of the maximum potential photosynthetic activity (Strasser et al., 2000), increased significantly in the middle of the experiment in the terrestrial runoff treatment, further suggesting an increase in photosynthetic efficiency under light attenuation induced by the runoff. Moreover, this mismatch between oxygen production and carbon fixation, which has already been reported in a mesocosm experiment in Antarctic coastal waters (Deppeler et al., 2018), might be explained by the fact that photosynthetic carbon fixation is a two-stage process. The first is the conversion of light to energy in the chloroplast, which produces oxygen as a by-product, and the second is the use of the produced energy to convert carbon dioxide into sugars through the Calvin cycle with the RuBisCO enzyme. Under stress conditions, the energy produced can also be used in alternative pathways and not carbon dioxide conversion – that is, mainly respiration and photoacclimation (Behrenfeld et al., 2004; Halsey et al., 2010). Hence, we hypothesized that in the runoff treatment, a significant part of the energy produced by photosynthesis was not converted to growth but was used instead in alternative pathways, which explains the observed mismatch between oxygen production and phytoplankton biomass. An alternative hypothesis is that the high quantity of particulate matter added through the simulated runoff induced a strong sedimentation of a part of the phytoplankton community toward the bottom of the mesocosm enclosures (Kiorboe et al., 1990). This sedimentation could have partly contributed to the mismatch between GPP and Chl a, as sedimented phytoplankton could have continued to produce oxygen, while being undetected by both manual and sensor monitoring of Chl a. Such sedimentation has already been suggested after heavy loadings of terrestrial matter occurred during a natural flash flood event in Thau Lagoon, during which most of the microbial production may have been exported through sedimentation (Fouilland et al., 2012). Nonetheless, it should be noted that the samples of sedimented material in the sediment

traps are not fully analysed yet, thus preventing the characterization of the role of sedimentation in the responses of GPP and Chl *a* with certainty.

Simultaneously, community respiration was strongly enhanced (+53 %) by the simulated terrestrial runoff. In marine waters, planktonic bacterial respiration is generally assumed to represent a major part of community respiration (Robinson, 2008). In the present study, bacterial abundance was significantly enhanced by the runoff during the first part of the experiment (d2–d9), which is congruent with the higher respiration at that time. This suggests that higher bacterial abundances are certainly responsible for the higher *R* reported in the runoff treatment during the first part of the experiment. However, bacterial abundances then significantly decreased during the middle of the experiment (d9–d14) in the runoff treatment, while respiration remained significantly higher than in the control treatment, resulting in a positive response of *R* normalized by bacterial abundance at this time of the experiment. This suggests that respiration was mostly not sustained by bacteria at that time of the experiment but by other biological compartments instead. Because Chl *a* was still strongly depressed by the runoff during this period of the experiment, resulting in extremely high CR : Chl *a* rates, the hypothesis of an increase in phytoplankton respiration is not plausible. An increase in zooplankton respiration might instead explain the positive effect on community respiration, as the abundance of some groups of metazooplankton was significantly enhanced by the runoff treatment (Courboulès et al., 2023), and the concomitant increase in PO_4^{3-} suggests a strong phosphorus excretion from zooplankton (Andersen et al., 1986; Vadstein et al., 1995).

As a consequence of the faster and greater increase in respiration compared to that in gross primary production, the terrestrial runoff resulted in a decrease in the production-to-respiration ratio and a shift toward heterotrophy of the metabolic index of the planktonic system during the first half of the experiment, as similarly reported after simulating a terrestrial runoff in a tropical reservoir (Trinh et al., 2016). Concomitantly, pCO_2 was significantly higher in the terrestrial runoff treatment, which was certainly because of the higher respiration as the responses of both variables were strongly correlated. These results are consistent with a study of 15 Swedish lakes that reported higher respiration leading to switches towards a heterotrophic metabolic index and increased pCO_2 in response to increased terrestrial carbon runoffs (Ask et al., 2012). Therefore, the present experiment shows, for the first time, to our knowledge, in Mediterranean coastal lagoons, that terrestrial runoffs could potentially shift coastal Mediterranean lagoons, such as the Thau Lagoon, from being net oxygen producers to net oxygen sinks in spring. Therefore, the respiration-driven gain in CO_2 can temporarily change the magnitude and direction of the air–sea CO_2 exchange, potentially switching the ecosystem from a CO_2 sink to a CO_2 source for the atmosphere.

4.2 Enhanced nutrient availabilities boosted phytoplankton processes during the second half of the experiment

During the second half of the experiment (d12–d18), the phytoplankton biomass and processes increased in the terrestrial runoff treatment in contrast to what occurred during the first half of the experiment. This might be explained by the higher dissolved inorganic nutrient availability in the runoff treatment, as both NH_4^+ and PO_4^{3-} concentrations were significantly higher in the terrestrial runoff treatment than in the control in the middle of the experiment before being consumed and returning to the control level. The higher NH_4^+ concentrations possibly resulted from bacterial remineralization, as NH_4^+ is mostly produced by the bacterial remineralization of organic matter in coastal waters (Nixon, 1981; Glibert, 1982). In contrast, the higher PO_4^{3-} availability could be linked to grazing on bacteria, as grazers feeding upon bacteria generally show high phosphorus excretion rates (Andersen et al., 1986).

Enhanced nutrient availability may have fuelled phytoplankton growth to such an extent that the positive effect of nutrient availability surpassed the negative effect of light attenuation. This result suggests a trade-off mechanism between light and nutrient availability, whereby phytoplankton metabolism is enhanced or depressed depending on the extent of nutrient enrichment compared to the light attenuation associated with terrestrial runoffs. This mechanism has already been reported for northern lakes (Klug, 2002; Isles et al., 2021) and even during mesocosm experiments evaluating the addition of dissolved organic matter into coastal waters of various regions (Deininger et al., 2016; Traving et al., 2017; Andersson et al., 2023). The present study provides additional support for this mechanism in Mediterranean coastal waters and highlights the importance of considering it when modelling their response to terrestrial runoffs.

As mentioned earlier, Chl *a* strongly increased during the second part of the experiment in the runoff treatment. This positive response was mainly due to an increase in the abundance of diatoms, mainly *Chaetoceros* and *Cylindrotheca*, Cyanobacteria, and autotrophic dinoflagellates (Courboulès et al., 2023). In addition, the pico- and nanophytoplankton abundances counted with flow cytometry also increased at this time of the experiment (Courboulès et al., 2023). Overall,đ very good agreement was found between the response of the Chl *a* concentration and phytoplankton abundances, measured by both microscopy and flow cytometry, during the entire experiment (Courboulès et al., 2023). The accumulation of phytoplankton biomass during the second part of the experiment in the runoff treatment was related to the strong increase in phytoplankton growth rate from d10, while the phytoplankton loss rate remained low until the end of the experiment. Consequently, the growth-to-loss ratio was significantly enhanced by more than 10 times compared to that of the control. This suggests an uncoupling between phy-

toplankton growth and its loss factors, such as zooplankton and/or viruses, at that time in the experiment, possibly because phytoplankton grew too quickly compared to its predators. Nonetheless, this emphasizes the potentially substantial structural impacts of terrestrial runoff on plankton communities and their intricate interactions within aquatic food webs as was recently documented in lakes (Strandberg et al., 2023).

The results of the present experiment suggest that the climate-change-related intensification of terrestrial runoffs could temporarily alter metabolic and trophic indices of the water column of the lagoon during productive seasons (Trombetta et al., 2019), potentially shifting it towards heterotrophy and disrupting its trophic balance. Coupled with terrestrial-runoff-induced shifts in microbenthic net community production towards heterotrophy (Liess et al., 2015), these alterations could interact with ongoing shifts occurring in the lagoon, such as the changes in trophic functioning towards mixotrophy and heterotrophy related to oligotrophication (Derolez et al., 2020b). Such consequences may also be seen in other Mediterranean lagoons, as turbidity and extreme flood events were reported to control phytoplankton abundance and phenology in oligotrophic Mediterranean coastal lagoons in southern France and Corsica (Bec et al., 2011; Ligorini et al., 2022). Even though the results of the present study come from a single mesocosm experiment, implying that their generalization should be implemented with care, they emphasize the importance of considering the effects of terrestrial runoffs on plankton-mediated processes in modelling projections of Mediterranean coastal waters under future climate scenarios.

Data availability. The data used in this paper are openly available in the Sea Scientific Open Data Edition (SEANOE) repository at https://www.seanoe.org/data/00861/97260/, last access: 22 March 2024 (Soulié et al., 2023).

Supplement. The supplement related to this article is available online at: https://doi.org/10.5194/bg-21-1887-2024-supplement.

Author contributions. FrV and BM designed the mesocosm experiment, and FrV, SM, and BM managed it. FrV, JC, MH, SM, FlV, CC, FJ, and BM participated in the daily samplings of the experiment. CC performed the analysis of pH, pCO_2, and dissolved inorganic carbon, with the help of FlV. TS processed the sensor data, made all related analyses, and wrote the original draft of the paper, with inputs from all authors. All authors read and approved the final version of the paper.

Competing interests. The contact author has declared that none of the authors has any competing interests.

Disclaimer. Publisher's note: Copernicus Publications remains neutral with regard to jurisdictional claims made in the text, published maps, institutional affiliations, or any other geographical representation in this paper. While Copernicus Publications makes every effort to include appropriate place names, the final responsibility lies with the authors.

Acknowledgements. We thank David Parin, Romain Michel, Hervé Violette, Kilian Terrier, Inès Garcia, Valentin Kempf, and Paul Verzele from MEDIMEER for their help with the mesocosm and sensor setup, daily sampling, and analyses of chemical variables. We acknowledge Eftihis Nikiforakis for his help with discrete oxygen measurements and daily sampling. We also thank David Pecqueur from the SU/CNRS BioPIC Imaging and OOB Cytometry platform and Barbara Marie from the Observatoire Océanologique de Banyuls-sur-Mer for the cytometric and the dissolved organic carbon analyses, respectively. We are grateful to Valerio Caruso from CNR-ISMAR for his valuable help in performing the total alkalinity analysis. We also thank the staff from the Puéchabon state forest for their help with practicalities during the sampling of soil. This work was part of the RESTORE project funded by the French National Research Agency under grant no. ANR-19-CE32-0013. Carolina Cantoni was funded as part of the Transnational Access project of AQUACOSM-plus, which received funding from the European Union's Horizon 2020 research and innovation programme under grant agreement no. 871081. As Carolina Cantoni is a member of the JERICO-S3 project, which received funding from the European Union's Horizon 2020 research and innovation programme under grant agreement nos. 871153 and 951799, her contribution to this work is also part of her contribution to JERICO-S3.

Financial support. This research has been supported by the Agence Nationale de la Recherche (grant no. ANR-19-CE32-0013) and Horizon 2020 (grant nos. 871081, 871153, and 951799).

Review statement. This paper was edited by Frédéric Gazeau and reviewed by Aurore Regaudie de Gioux and Tamara Cibic.

References

Allard, V., Ourcival, J. M., Rambal, S., Joffre, R., and Rocheteau, A.: Seasonal and annual variation of carbon exchange in an evergreen Mediterranean forest in southern France, Glob. Change Biol., 14, 714–725, https://doi.org/10.1111/j.1365-2486.2008.01539.x, 2008.

Aminot, A., Kirkwood, D. S., and Kérouel R.: Determination of ammonia in seawater by the indophenol-blue method: Evaluation of the ICES NUTS I/C 5 questionnaire, Mar. Chem., 56, 59–75, https://doi.org/10.1016/S0304-4203(96)00080-1, 1997.

Aminot, A. and Kérouel R.: Dosage automatique des nutriments dans les eaux marines, Méthodes en flux continu, edited by: Ifremer, Q., 336 pp., ISBN 2-84433-133-5, 2007.

Andersen, O. K., Goldman, J. C., Caron, D. A., and Dennett, M. R.: Nutrient cycling in a microflagellate food chain: III. Phosphorus dynamics, Mar. Ecol. Prog. Ser., 31, 47–55, 1986.

Andersson, A., Brugel, S., Paczkowska, J., Rowe, O. F., Figueroa, D., Kratzer, S., and Legrand, C.: Influence of allochthonous dissolved organic matter on pelagic basal production in a northerly estuary, Estuar. Coast. Shelf Sci., 204, 225–235, https://doi.org/10.1016/j.ecss.2018.02.032, 2018.

Andersson, A., Grinienė, E., Berglund, A. M. M., Brugel, S., Gorokhova, E., Figueroa, D., Gallampois, C., Ripszam, M., and Tysklind, M.: Microbial food web changes induced by terrestrial organic matter and elevated temperature in the coastal northern Baltic Sea, Front. Mar. Sci., 10, 1170054, https://doi.org/10.3389/fmars.2023.1170054, 2023.

Alpert, P., Ben-Gai, T., Baharad, A., Benjamini, Y., Yekutieli, D., Colacino, M., Diodato, L., Ramis, C., Homar, V., Romero, R., Michaelides, S., and Manes, A.: The paradoxical increase of Mediterranean extreme daily rainfall in spite of decrease in total values, Geophys. Res. Lett., 29, 31-1–31-4. https://doi.org/10.1029/2001GL013554, 2002.

Ask, J., Karlsson, J., and Jansson, M.: Net ecosystem production in clear-water and brown-water lakes, Global Biogeochem. Cyc., 26, GB1017, https://doi.org/10.1029/2010GB003951, 2012.

Bec, B., Collos, Y., Souchu, P., Vaquer, A., Lautier, J., Fiandrino, A., Benau, L., Orsoni, V., and Laugier, T.: Distribution of picophytoplankton and nanophytoplankton along an anthropogenic eutrophication gradient in French Mediterranean coastal lagoons, Aquat. Microb. Ecol., 63, 29–45, https://doi.org/10.3354/ame01480, 2011.

Behrenfeld, M. J., Prasil, O., Babin, M., and Bruyant, F.: In search of a physiological basis for covariations in light limited and light saturated photosynthesis, J. Phycol., 40, 4–25, https://doi.org/10.1046/j.1529-8817.2004.03083.x, 2004.

Blanchet, C. C., Arzel, C., Davranche, A., Kahilainen, K. K., Secondi, J., Taipale, S., Lindberg, H., Loehr, J., Manninen-Johansen, S., Sundell, J., Maanan, M., and Nummi, P.: Ecology and extent of freshwater browning – What we know and what should be studied next in the context of global change, Sci. Total Environ., 812, 152420, https://doi.org/10.1016/j.scitotenv.2021.152420, 2022.

Brussaard, C. P. D.: Viral control of phytoplankton populations – a review, J. Eukaryot. Microbiol., 51, 125–138, https://doi.org/10.1111/j.1550-7408.2004.tb00537.x, 2004.

Carrit, D. E. and Carpenter, J. H.: Comparison and evaluation of currently employed modifications of the Winkler method for determining oxygen in seawater, A NASCO report, J. Mar. Res., 24, 286–318, 1966.

Clayton, T. D. and Byrne, R. H.: Spectrophotometric seawater pH measurements: Total hydrogen ion concentration scale calibration of m-cresol purple and at-sea results, Deep-Sea Res. Pt. I, 40, 2115–2129, https://doi.org/10.1016/0967-0637(93)90048-8, 1993.

Courboulès, J., Vidussi, F., Soulié, T., Mas, S., Pecqueur, D., and Mostajir, B.: Effects of experimental warming on small phytoplankton, bacteria and viruses in autumn in the Mediterranean coastal Thau lagoon, Aquat. Ecol., 55, 647–666, https://doi.org/10.1007/s10452-021-09852-7, 2021.

Courboulès, J., Vidussi, F., Soulié, T., Nikiforakis, E., Heydon, M., Mas, S., Joux, F., and Mostajir, B.: Effects of an experimental terrestrial runoff on the components of the plankton food web in a Mediterranean coastal lagoon, Font. Mar. Sci., 10, 1200757, https://doi.org/10.3389/fmars.2023.1200757, 2023.

Deininger, A., Faithfull, C. L., Lange, K., Bayer, T., Vidussi, F., and Liess, A.: Simulated terrestrial runoff triggered a phytoplankton succession and changed stoichiometry in coastal lagoon mesocosms, Mar. Environ. Res., 119, 40–50, https://doi.org/10.1016/j.marenvres.2016.05.001, 2016.

Deininger, A. and Frigstad, H.: Reevaluating the role of organic matter sources for coastal eutrophication, oligotrophication, and ecosystem health, Front. Mar. Sci., 6, 210, https://doi.org/10.3389/fmars.2019.00210, 2019.

Deppeler, S., Petrou, K., Schulz, K. G., Westwood, K., Pearce, I., McKinlay, J., and Davidson, A.: Ocean acidification of a coastal Antarctic marine microbial community reveals a critical threshold for CO_2 tolerance in phytoplankton productivity, Biogeosciences, 15, 209–231, https://doi.org/10.5194/bg-15-209-2018, 2018.

Derolez, V., Soudant, D., Malet, N., Chiantella, C., Richard, M., Abadie, E., Aliaume, C., and Bec, B.: Two decades of oligotrophication: evidence for a phytoplankton community shift in the coastal lagoon of Thau (Mediterranean Sea, France), Estuar. Coast. Shelf Sci., 241, 106810, https://doi.org/10.1016/j.ecss.2020.106810, 2020a.

Derolez, V., Malet, N., Fiandrino, A., Lagarde, F., Richard, M., Ouisse, V., Bec, B., and Aliaume, C.: Fifty years of ecological changes: Regime shifts and drivers in a coastal Mediterranean lagoon during oligotrophication, Sci. Total Environ., 732, 139292, https://doi.org/10.1016/j.scitotenv.2020.139292, 2020b.

Dickson, A. G.: Standard potential of the reaction: AgCl(s) + 1 2H2(g) = Ag(s) + HCl (aq), and the standard acidity constant of the ion HSO_4 – in synthetic sea water from 273.15 to 318.15 K, J. Chem. Thermodyn., 22, 113–127, https://doi.org/10.1016/0021-9614(90)90074-Z, 1990.

Dickson, A. G., Sabine, C. L., Christian, J. R., and North Pacific Marine Science Organization: Guide to best practices for ocean CO_2 measurements, North Pacific Marine Science Organization, https://www.oceanbestpractices.net/handle/11329/249 (last access: 13 September 2023), 2007.

Ducrocq, V., Nuissier, O., Ricard, D., Lebeaupin, C., and Thouvenin, T.: A numerical study of three catastrophic precipitating events over southern France, II: Mesoscale triggering and stationary factors, Q. J. R. Meteorol. Soc., 134, 131–145, https://doi.org/10.1002/qj.199, 2008.

Falkowski, P. G., Laws, E. A., Barber, R. T., and Murray, J. W.: Phytoplankton and their role in primary, new and export production, in: Ocean Biogeochemistry. Global Change – The IGBP Series (closed), edited by: Fasham, M. J. R., Springer, Berlin, Heidelberg, https://doi.org/10.1007/978-3-642-55844-3_5, 2003.

Falkowski, P.: Ocean science: the power of plankton, Nature, 483, S17–S20, https://doi.org/10.1038/483S17a, 2012.

Fouilland, E., Trottet, A., Bancon-Montigny, C., Bouvy, M., Le Floc'h, E., Gonzalez, J. L., Hatey, E., Mas, S., Mostajir, B., Nouguier, J., Pecqueur, D., Rochelle-Newall, E., Rodier, C., Roques, C., Salles, C., Tournoud, M.-G., and

Vidussi, F.: Impact of a river flash flood on microbial carbon and nitrogen production in a Mediterranean lagoon (Thau lagoon, France), Estuar. Coast. Shelf Sci., 113, 192–204, https://doi.org/10.1016/j.ecss.2012.08.004, 2012.

Giller, P. S., Hillebrand, H., Berninger, U.-G., Gessner, M. O., Hawkins, S., Inchausti, P., Inglis, C., Leslie, H., Malmqvist, B., Monaghan, M. T., Morin, P. J., and O'Mullan, G.: Biodiversity effects on ecosystem functioning: emerging issues and their experimental test in aquatic environments, Oikos, 104, 423–436, https://doi.org/10.1111/j.0030-1299.2004.13253.x, 2004.

Glibert, P. M.: Regional studies of daily, seasonal and size fraction variability in ammonium remineralization, Mar. Biol., 70, 209–222, https://doi.org/10.1007/BF00397687, 1982.

Halsey, K. H., Milligan, A. J., and Behrenfeld, M. J.: Physiological optimization underlies growth rate-independent chlorophyll-specific gross and net primary production, Photosynth. Res., 103, 125–137, https://doi.org/10.1007/s11120-009-9526-z, 2010.

Hernández-Ayón, J. M., Belli, S. L., and Zirino, A.: pH, alkalinity and total CO_2 in coastal seawater by potentiometric titration with a difference derivative readout, Anal. Chim. Acta, 394, 101–108, https://doi.org/10.1016/S0003-2670(99)00207-X, 1999.

Holmes, R. M., Aminot, A., Kérouel, R., Hooker, B. A., and Peterson, B. J.: A simple and precise method for measuring ammonium in marine and freshwater ecosystems, Can. J. Fish. Aq. Sci., 56, 1801–1808, https://doi.org/10.1139/f99-128, 1999.

Isles, P. D. F., Creed, I. F., Jonsson, A., and Bergström, A.-K.: Trade-offs between light and nutrient availability across gradients of dissolved organic carbon lead to spatially and temporally variable responses of lake phytoplankton biomass to browning, Ecosystems, 24, 1837–1852, https://doi.org/10.1007/s10021-021-00619-7, 2021.

Kiorboe, T., Andersen, K. P., and Dam, H. G.: Coagulation efficiency and aggregate formation in marine phytoplankton, Mar. Biol., 107, 235–245, https://doi.org/10.1007/BF01319822, 1990.

Klug, J. L.: Positive and negative effects of allochthonous dissolved organic matter and inorganic nutrients on phytoplankton growth, Can. J. Fish. Aquat. Sci., 59, 85–95, https://doi.org/10.1139/f01-194, 2002.

La Jeunesse, I., Cirelli, C., Sellami, H., Aubin, D., Deidda, R., and Baghdadi, N.: Is the governance of the Thau coastal lagoon ready to face climate change impacts?, Ocean Coast. Manag., 118, 234–246, https://doi.org/10.1016/j.ocecoaman.2015.05.014, 2015.

Landry, M. R. and Hassett, R. P.: Estimating the grazing impact of marine micro-zooplankton, Mar. Biol., 67, 283–288,. https://doi.org/10.1007/BF00397668, 1982.

Lee, K., Kim, T.-W., Byrne, R. H., Millero, F. J., Feely, R. A., and Liu, Y.-M.: The universal ratio of boron to chlorinity for the North Pacific and North Atlantic oceans, Geochim. Cosmochim. Ac., 74, 1801–1811, https://doi.org/10.1016/J.GCA.2009.12.027, 2010.

Legendre, L. and Rassoulzadegan, F.: Plankton and nutrient dynamics in marine waters, Ophelia, 41, 153–172, https://doi.org/10.1080/00785236.1995.10422042, 1995.

Lewis, E. and Wallace, D. W. R.: Program Developed for CO_2 System Calculations, ORNL/CDIAC-105. Carbon Dioxide Information Analysis Center, Oak Ridge, TN, Oak Ridge National Laboratory, U.S, Department of Energy, https://doi.org/10.15485/1464255, 1998.

Liess, A, Faithfull, C., Reichstein, B., Rowe, O., Guo, J., Pete, R., Thomsson, G., Uszko W., and Francoeur, S. N.: Terrestrial runoff may reduce microbenthic net community productivity by increasing turbidity: a Mediterranean coastal lagoon mesocosm experiment, Hydrobiologia, 753, 205–218, https://doi.org/10.1007/s10750-015-2207-3, 2015.

Liess, A., Rowe, O., Francoeur, S. N., Guo, J., Lange, K., Schröder, A., Reichstein, B., Lefèbure, R., Deininger, A., Mathisen, P., and Faithfull, C. L.: Terrestrial runoff boosts phytoplankton in a Mediterranean coastal lagoon, but these effects do not propagate to higher trophic levels, Hydrobiologia, 766, 275–291, https://doi.org/10.1007/s10750-015-2461-4, 2016.

Ligorini, V., Malet, N., Garrido, M., Derolez, V., Amand, M., Bec, B., Cecchi, P., and Pasqualini, V.: Phytoplankton dynamics and bloom events in oligotrophic Mediterranean lagoons: seasonal patterns but hazardous trends, Hydrobiologia, 849, 2353–2375, https://doi.org/10.1007/s10750-022-04874-0, 2022.

Liu, X., Patsavas, M. C., and Byrine, R. H.: Purification and characterization of meta-cresol purple for spectrophotometric seawater pH measurements, Environ. Sci. Technol., 45, 4862–4868, https://doi.org/10.1021/es200665d, 2011.

Lopez-Urrutia, A., Martin, E. S., Harris, R. P., and Irigoien, X.: Scaling the metabolic balance of the oceans, P. Natl. Acad. Sci. USA, 103, 8739–8744, https://doi.org/10.1073/pnas.0601137103, 2006.

Lueker, T. J., Dickson, A. G., and Keeling, C. D.: Ocean pCO_2 calculated from dissolved inorganic carbon, alkalinity, and equations for K_1 and K_2: validation based on laboratory measurements of CO_2 in gas and seawater at equilibrium, Mar. Chem., 70, 105–119, https://doi.org/10.1016/S0304-4203(00)00022-0, 2000.

Marie, D., Partensky, F., Jacquet, S., and Vaulot, D.: Enumeration and cell cycle analysis of natural populations of marine picoplankton by flow cytometry using the nucleic acid stain SYBR Green I, Appl. Environ. Microbiol., 63, 186–193, https://doi.org/10.1128/AEM.63.1.186-193.1997, 1997.

Meunier, C., Liess, A., Andersson, A., Brugel, S., Paczkowska, J., Rahman, H., Skoglund, B., and Rowe, O. F.: Allochthonous carbon is a major driver of the microbial food web – A mesocosm study simulating elevated terrestrial matter runoff, Mar. Environ. Res., 129, 236–244, https://doi.org/10.1016/j.marenvres.2017.06.008, 2017.

Mostajir, B., Amblard, C., Buffan-Dubau, E., de Wit, R., Lensi, R., and Sime-Ngando, T.: Microbial food webs in aquatic and terrestrial ecosystems, in: Environmental Microbiology: Fundamentals and Applications, edited by: Bertrand, J.-C., Caumette, P., Lebaron, P., Normand, P., andSime-Ngando, T., Springer, the Netherlands, Chap. 13, 458–509, https://doi.org/10.1007/978-94-017-9118-2_13, 2015.

Müller, O., Seuthe, L., Bratbak, G., and Paulsen, M. L.: Bacterial response to permafrost derived organic matter input in an Arctic fjord, Front. Mar. Sci., 5, 263, https://doi.org/10.3389/fmars.2018.00263, 2018.

Mustaffa, N., Kallajoki, L., Biederbick, J., Binder, F., Schlenker, A., and Striebel, M.: Coastal ocean darkening effects via terrigenous DOM addition on plankton: an indoor mesocosm experiment, Front. Mar. Sci., 7, 547829, https://doi.org/10.3389/fmars.2020.547829, 2020.

Nixon, S. W.: Remineralization and nutrient cycling in coastal marine ecosystems, in: Estuaries and nutrients, Contemporary Issues in Science and Society, edited by: Neilson, B. J. and Cronin, L. E., Humana Press, https://doi.org/10.1007/978-1-4612-5826-1_6, 1980.

Nunes, J. P., Seixas, J., Keizer, J. J., and Ferreira, A. J. D.: Sensitivity of runoff and soil erosion to climate change in two Mediterranean watersheds, Part I: model parameterization and evaluation, Hydrol. Process., 23, 1202e1211, https://doi.org/10.1002/hyp.7247, 2009.

Paczkowska, J., Brugel, S., Rowe, O., Lefébure, R., Brutemark, A., and Andersson, A.: Response of coastal phytoplankton to high inflows of terrestrial matter, Front. Mar. Sci., 7, 80, https://doi.org/10.3389/fmars.2020.00080, 2020.

Pecqueur, D., Vidussi, F., Fouilland, E., Le Floc'h, E., Mas, S., Roques, C., Salles, C., Tournoud, M.-G., and Mostajir, B.: Dynamics of microbial planktonic food web components during a river flash flood in a Mediterranean coastal lagoon, Hydrobiologia, 673, 13–27, https://doi.org/10.1007/s10750-011-0745-x, 2011.

Pierrot, D. E., Lewis, D., and Wallace, W. R.: MS Excel Program Developed for CO_2 System Calculations, ORNL/CDIAC-105a, Oak Ridge, Tennessee, Carbon Dioxide Information Analysis Center, Oak Ridge National Laboratory, U.S. Department of Energy, https://doi.org/10.3334/CDIAC/otg.CO2SYS_XLS_CDIAC105a, 2006.

Plus, M., La Jeunesse, I., Bouraoui, F., Zaldivar, J.-M., Chapelle, A., and Lazure, P.: Modelling water discharges and nitrogen inputs into a Mediterranean lagoon: Impact on the primary production, Ecol. Modell., 193, 69–89, https://doi.org/10.1016/j.ecolmodel.2005.07.037, 2006.

Robinson, C.: Heterotrophic bacterial respiration, in: Microbial Ecology of the Oceans, 2nd Edn., edited by: Kirchman, D. L., Hoboken, NJ, Wiley, 299–334, 2008.

Sanchez, E., Gallardo, C., Gaertner, M. A., Arribas, A., and Castro, M.: Future climate extreme events in the Mediterranean simulated by a regional climate model: a first approach, Glob. Planet. Change, 44, 163e180, https://doi.org/10.1016/j.gloplacha.2004.06.010, 2004.

Scharnweber, K., Peura, S., Attermeyer, K., Bertilsson, S., Bolender, L., Buck, M., Einarsdóttir, K., Garcia, S. L., Gollnisch, R., Grasset, C., Groeneveld, M., Hawkes, J. A., Lindström, E. S., Manthey, C., Övergaard, R., Rengefors, K., Sedano-Núñez, V. T., Tranvik, L. J., and Székely, A. J.: Comprehensive analysis of chemical and biological problems associated with browning agents used in aquatic studies, Limnol. Oceanogr. Method., 19, 818–835, https://doi.org/10.1002/lom3.10463, 2021.

Soria, J., Pérez, R., and Soria-Pepinya, X.: Mediterranean coastal lagoons review: Sites to visit before disappearance, J. Mar. Sci. Eng., 10, 347, https://doi.org/10.3390/jmse10030347, 2022.

Soulié, T., Mas, S., Parin, D., Vidussi, F., and Mostajir, B.: A new method to estimate planktonic oxygen metabolism using high-frequency sensor measurements in mesocosm experiments and considering daytime and nighttime respirations, Limnol. Oceanogr. Method., 19, 303–316, https://doi.org/10.1002/lom3.10424, 2021.

Soulié, T., Vidussi, F., Mas, S., and Mostajir, B.: Functional stability of a coastal Mediterranean plankton community during an experimental marine heatwave, Front. Mar. Sci., 9, 831496, https://doi.org/10.3389/fmars.2022.831496, 2022a.

Soulié, T., Stibor, H., Mas, S., Braun, B., Knechtel, J., Nejstgaard, J. C., Sommer, U., Vidussi, F., and Mostajir, B.: Brownification reduces oxygen gross primary production and community respiration and changes the phytoplankton community composition: an in situ mesocosm experiment with high-frequency sensor measurements in a North Atlantic Bay, Limnol. Oceanogr., 67, 874–887, https://doi.org/10.1002/lno.12041, 2022b.

Soulié, T., Vidussi, F., Courboulès, J., Heydon, M., Mas, S., Voron, F., Cantoni, C., Joux, F., and Mostajir, B.: Dataset from a mesocosm experiment testing the effects of a terrestrial runoff on a Mediterranean plankton community, SEANOE [data set], https://doi.org/10.17882/97260, 2023.

Staehr, P. A., Bade, D., de Bogert, M. C. V., Koch, G. R., Williamson, C., Hanson, P., Cole, J. J., and Kratz, T.: Lake metabolism and the diel oxygen technique: state of the science, Limnol. Oceanogr. Method., 8, 628–644, https://doi.org/10.4319/lom.2010.8.0628, 2010.

Strandberg, U., Hiltunen, M., Creed, I. F., Arts, M. T., and Kankaala, P.: Browning-induced changes in trophic functioning of planktonic food webs in temperate and boreal lakes: insights from fatty acids, Oecologia, 201, 183–197, https://doi.org/10.1007/s00442-022-05301-w, 2023.

Strasser, R. J., Srivastava, A., and Tsimilli-Michael, M.: The fluorescence transient as a tool to characterize and screen photosynthetic samples, in: Probing photosynthesis: Mechanisms, regulation and adaptation, edited by: Yunus, M., Pathre, U., and Mohanty, P., Taylor and Francis, UK, CRC Press, 445–483, ISBN: 1482268019, 9781482268010, 2000.

Striebel, M., Kallajoki, L., Kunze, C., Wollschläger, J., Deininger, A., and Hillebrand, H.: Marine primary producers in a darker future: a meta-analysis of light effects on pelagic and benthic autotrophs, Oikos, 2023, e09501, https://doi.org/10.1111/oik.09501, 2023.

Traving, S. J., Rowe, O., Jakobsen, N. M., Sorensen, H., Dinasquet, J., Stedmon, C. A., Andersson, A., and Riemann, L.: The effect of increased loads of dissolved organic matter on estuarine microbial community composition and function, Front. Microb., 8, 351, https://doi.org/10.3389/fmicb.2017.00351, 2017.

Trinh, D. A., Minh Luu, T. N., Trinh, Q. H., Tran, H. S., Tran, T. M., Quynh Le, T. P., Duong, T. T., Orange, D., Janeau, J. L., Pommier, T., and Rochelle-Newall, E.: Impact of terrestrial runoff on organic matter, trophic state, and phytoplankton in a tropical, upland reservoir, Aquat. Sci., 78, 367–379, https://doi.org/10.1007/s00027-015-0439-y, 2016.

Trombetta, T., Vidussi, F., Mas, S., Parin, D., Simier, M., and Mostajir, B.: Water temperature drives phytoplankton blooms in coastal waters, Plos ONE, 14, e0214933, https://doi.org/10.1371/journal.pone.0214933, 2019.

Vadstein, O., Brekke, O., Andersen, T., and Olsen, Y.: Estimation of phosphorus release rates from natural zooplankton communities feeding on planktonic algae and bacteria, Limnol. Oceanogr., 40, 250–262, https://doi.org/10.4319/lo.1995.40.2.0250, 1995.

Zapata, M., Rodriguez, F., and Garrido, J. L.: Separation of chlorophylls and carotenoids from marine phytoplankton: a new HPLC method using a reversed phase C_8 column and pyridine-containing mobile phases, Mar. Ecol. Prog. Ser., 195, 29–45, https://doi.org/10.3354/meps195029, 2000.